# Prediction of parameters related to grape ripening by multivariate calibration of voltammetric signals acquired by an electronic tongue

L. Pigani, G. Vasile Simone, G. Foca, A. Ulrici, F. Masino, L. Cubillana-Aguilera, R. Calvini, R. Seeber


www.elsevier.com/locate/talanta

PII: S0039-9140(17)30970-0
DOI: http://dx.doi.org/10.1016/j.talanta.2017.09.027
Reference: TAL17930

To appear in: *Talanta*

Received date: 16 June 2017
Revised date: 7 September 2017
Accepted date: 10 September 2017

Cite this article as: L. Pigani, G. Vasile Simone, G. Foca, A. Ulrici, F. Masino, L. Cubillana-Aguilera, R. Calvini and R. Seeber, Prediction of parameters related to grape ripening by multivariate calibration of voltammetric signals acquired by an electronic tongue, *Talanta,* http://dx.doi.org/10.1016/j.talanta.2017.09.027

# Prediction of parameters related to grape ripening by multivariate calibration of voltammetric signals acquired by an electronic tongue

L. Pigani[1,2*], G. Vasile Simone[1,2], G. Foca[2,3], A. Ulrici[2,3], F. Masino[2,3], L. Cubillana-Aguilera[4], R. Calvini[2], R. Seeber[1,2]

[1]Dipartimento di Scienze Chimiche e Geologiche, Università degli Studi di Modena e Reggio Emilia, Via G. Campi, 103 – 41125 Modena

[2]Centro Interdipartimentale BIOGEST-SITEIA, Università di Modena e Reggio Emilia, Padiglione Besta, Via Amendola, 2 – 42122 Reggio Emilia

[3]Dipartimento di Scienze della Vita, Università di Modena e Reggio Emilia, Padiglione Besta, Via Amendola, 2 – 42122 Reggio Emilia

[4]Institute of Research on Electron Microscopy and Materials, Department of Analytical Chemistry, Faculty of Sciences, Campus de Excelencia Internacional del Mar, University of Cadiz, República Saharaui, S/N. 11510 Puerto Real, Cadiz-Spain.

*laura.pigani@unimore.it



**Abstract**

An electronic tongue (ET) consisting of two voltammetric sensors, namely a poly-ethylendioxythiophene modified Pt electrode and a sonogel carbon electrode, has been developed aiming at monitoring grape ripening. To test the effectiveness of device and measurement procedures developed, samples of three varieties of grapes have been collected from veraison to harvest of the mature grape bunches. The derived musts have been then submitted to electrochemical investigation using Differential Pulse Voltammetry technique. At the same time, quantitative determination of specific analytical parameters for the evaluation of technological and phenolic maturity of each sample

has been performed by means of conventional analytical techniques. After a preliminary inspection by principal component analysis, calibration models were calculated both by partial least squares (PLS) on the whole signals and by the interval partial least squares (iPLS) variable selection algorithm, in order to estimate physico-chemical parameters. Calibration models have been obtained both considering separately the signals of each sensor of the ET, and by proper fusion of the voltammetric data selected from the two sensors by iPLS. The latter procedure allowed us to check the possible complementarity of the information brought by the different electrodes. Good predictive models have been obtained for estimation of pH, total acidity, sugar content, and anthocyanins content. The application of the ET for fast evaluation of grape ripening and of most suitable harvesting time is proposed.



**Keywords**

Voltammetric sensors; electronic tongue; grape ripening; partial lest squares regression; variable selection; data fusion.

## 1. Introduction

The development of analytical procedures for the assessment of fruit quality, requiring simple instrumentation and allowing rapid execution of reliable measurements, is of basic importance in several steps of the production chain. The whole path ranges from the selection of the best harvest time to the definition of the storage conditions [1,2]. In this frame, monitoring the ripening of grapes (*Vitis vinifera*) constitutes the essential tool for planning most proper harvest time; in fact, the final oenological result depends primarily on the assessment of grape ripeness. For the evaluation of the different indicators defining what is conventionally called technological, phenolic, and aromatic maturity, the quantitative determination of specific analytical data, including the content of sugars and acids, as well of polyphenols and aroma compounds, is necessary.

In this context, the application of sensing systems to the *in situ* study of real matrices, requiring minimal or no manipulation of the sample at all, is a very urgent task. The final goal consists in the quantitative determination of one or more analytes, or in the estimation of overall quality parameters, also related to the sensory characteristics, such as ‘smell’, ‘taste’ and ‘colour’. To such an aim, the

development of devices known as electronic noses (ENs) [3,4], electronic tongues (ETs) [5,6] and electronic eyes (EEs) [7,8] is of chief importance to obtain fast and objective indications.

When using ENs, ETs and EEs, the approach followed for the determination of the parameters of interest is based on 'blind analysis' techniques. In blind analysis no assumption about the species responsible for the measured signals is necessary: the information sought is extracted from the pattern of responses of the set of used sensors, through suitable chemometric treatments. In this context also the matrix effect on the responses, which is usually a drawback, may constitute an additional source of useful information, once reproducible. Matrix effects, in fact, affect differently the signals due to characteristic of the matrix itself, although the component of the matrix are not directly monitored. Moreover, the combination of data acquired by ETs, ENs and EEs, through proper data fusion techniques, can furnish more accurate information than any one of the individual sensing devices [9].

In this frame, our activity is devoted to collect and elaborate the data coming from a sensing system consisting of an EE and an ET in order to estimate the ripening of three purple grape varieties. The idea behind these studies is to investigate the possibility to develop a device able to easily quantify the parameters that are generally used to estimate both the technological and the phenolic maturity. The former one is typically related to the content of acids and sugars, while the latter one is associated to the amount of polyphenols. Among these last species, anthocyanins are most interesting in the case of grapes used for the production of red wines.

In particular, the present paper reports the results concerning the use of an ET in the analysis of grape samples at different maturation levels. It must be mentioned that a further research work is in progress on the same samples, devoted to evaluate the effectiveness of an EE to the same purpose. With respect to reported applications of ETs to similar issues [10], our approach differs as to the used sensing elements, as to the electrochemical technique adopted for the acquisition of the signals, as to the data elaboration strategies and as to the number of distinctive parameters. In particular, let's cite those connected to the polyphenolic content considered for the construction of the multivariate calibration models.

Sensors based on electrochemical transduction have been used as sensing elements in ET for the analysis of food matrices, thanks to the notable advantages due to the use of low-cost electrochemical instrumentation, which can be easily embedded in miniaturized systems [11-15]. The ET used in this study consists of two different voltammetric sensors, namely a Pt electrode modified by a conducting polymer and a sonogel carbon electrode. The different nature of the electrode materials supposedly leads to responses bringing different, partially complementary information. Some of us have previously

evidenced the advantages offered by the use of conducting polymers as modifying materials of the electrode surfaces in ETs employed in recognition of different kinds of fruit juices [16], and in discrimination of different white and red wines with respect to variety, geographical origin and other characteristics of interest [17-19]. In these studies, we verified the effectiveness of a particular sensor, namely a Pt substrate coated by a poly-ethylendioxythiophene (PEDOT) film [16], which allowed faster and simpler measurements with respect to both bare and differently modified electrodes, also providing for an improved degree of cross-selectivity. The reproducibility of different PEDOT electrodes, realised under the same experimental conditions, was testified by the coincidence of responses recorded on the same solutions.

In the present study, together with the PEDOT modified electrode (PEDOT-electrode), an electrode consisting of sonogel-carbon (SNGC-electrode) [20-22] has been also tested as a sensing element of the ET. As it is well known, carbon-based materials are most commonly used for detection of polyphenolic compounds [23-26], whose content varies notably during ripening of grapes. SNGC electrodes, prepared as described in ref. 22, are characterized by robustness, coupled to reduced dimensions and good electrochemical efficiency, particularly as to sensitivity, reproducibility and possible activation of electrocatalysis.

The electrochemical signals have been acquired using Differential Pulse Voltammetry (DPV) technique with the ET on grape samples collected at different ripening times. Then, the signals have been elaborated by means of proper chemometric techniques using a blind analysis approach that was already successfully applied for the analysis of fruit juices [16] and wines [17-19]. Calibration models for the prediction of the physicochemical parameters were developed by means of Partial Least Squares (PLS) and of interval-Partial Least Squares (iPLS) [27], both considering separately the electrochemical signals of the two voltammetric sensors, and by mid-level data fusion [28-30] of the features selected by iPLS on the two sensors.



## 2. Experimental

### *2.1 Samples*

Three Italian purple grape varieties, namely *Ancellotta* (A), *Lambrusco Marani* (L) and *Malbo Gentile* (M) were considered.

Samples were collected during vintage 2015, at 5 intervals of about 10 days (T0, T1, T2, T3, T4) from veraison to harvest of the mature grape bunches. For each grape variety three plants belonging to inner rows were marked. One hundred berries per plant were randomly picked at the base of pedicel for each harvest time. Samples were transferred at 4 °C to the laboratory and quickly brought in a form suitable to physico-chemical characterization and analysis by ET. The berries were crushed and macerated under nitrogen atmosphere, for one hour at 4°C in an enclosed container in the dark, to avoid air contact. The macerate was centrifuged under refrigerated conditions (4°C) at 4000 rpm for 15 min. The supernatant, called "must" from here onwards, was recovered and divided into different aliquots, in order to perform replicates for each determination. Finally, it was stored at -20 °C and each aliquot was unfrozen just before analysis.

Electrochemical and physico-chemical analyses were performed in parallel. Each must sample was analysed twice in two different acquisition sessions: the first time the acquisition order was randomized, then the order was shuffled and all the samples were analysed a second time. Thus, the overall number of analysed samples was equal to 45, requiring 90 analyses as a whole (3 grape varieties × 5 harvest times × 3 field replicates × 2 analytical replicates).

### *2.2 Physico-chemical characterization*

In order to estimate the grape ripeness, 18 physico-chemical parameters were determined on the must samples:

- total flavonoids content (TF) was determined by UV-Vis spectrophotometry (absorbance measured at $\lambda$ = 280 nm) and the result was expressed as mg of (+) catechin/L [31]. In this work, all the UV-Vis measurements were carried out using a Perkin Elmer Lambda 650 spectrophotometer equipped with a 10 mm quartz cuvette, and diluting the sample 50 times in hydrochloric acid-ethanol solution (ethanol:$H_2O$:HCl 70:30:1 v/v/v);
- total anthocyanins content (TAnt) was determined by UV-Vis spectrophotometry (absorbance measured at $\lambda$ = 540 nm) and the result was expressed as mg of oenin chloride/L [31];
- tonality (Ton) was calculated as the ratio between the absorbances at 420 nm (corresponding to a yellow-orange sample colour) and at 520 nm (corresponding to a red-purple sample colour). This parameter is commonly used in oenology to evaluate the oxidation of wine during aging [32]. In the present case, Ton was considered as a parameter suitable to describe the colour variation that occurs during grape ripening;

- colour index (CI) was calculated as the sum of the absorbance at 420 nm, 520 nm and 620 nm (the last one corresponding to a blue sample colour) [33]. In oenology, CI is used to assess the colour of red wines and to perform colour correction by addition of a blending wine up to the desired CI value;
- optical density (OD420%, OD520%, OD620%), defined as the percentage contribution of each absorbance, at 420, 520 and 620 nm, to CI [32];
- total polyphenols content (TP) was determined by following the Folin-Ciocalteu procedure reported in the OIV-MA-AS2-10 method [34]; the result has been expressed as mg of (+) catechin/L;
- the content of the five most abundant anthocyanins, i.e., 3-O-monoglucoside of delphinidin (Df-3-glc), cyanidin (Cn-3-glc), petunidin (Pt-3-glc), peonidin (Pn-3-glc), and malvidin (Mv-3-glc), was determined by reverse phase-high performance liquid chromatography, using a diode array detector (RP-HPLC-DAD). The method was described by Chinnici et al. [35] and adjusted as reported by Vasile Simone et al. [36]. Quantification was performed at fixed wavelength of 520 nm by Total-Chrom Workstation version 6.2.1 chromatographic system software (PerkinElmer, Inc.). The concentration of each compound was expressed as malvidin-3-O-glucoside equivalents;
- glucose (Glu) and fructose (Fru) were determined with the same chromatographic equipment used to determine anthocyanins. In this case, sugars were revealed by a refractive index detector (Series 200 refractive index detector, Perkin Elmer Inc.). As to the preparation of the sample, the musts (1 mL) were basified to pH 9–10 by NaOH 1 mol/L and then loaded into a 0.5 g-SAX cartridge (Isolute® SAX; Biotage), conditioned with 3 mL methanol and, subsequently, with 3 mL $H_2O$. Total sugars were eluted with 3 mL deionized $H_2O$ made up to final volume of 5 mL and filtered through 0.45 μm nylon filters before HPLC analysis. Samples were directly injected with a 5-μL loop using the above cited injection valve into a thermostated Phenomenex (Torrance) BIO-RAD Organic Acid Analysis Column (30 cm × 7.8 mm), at a column temperature of 50 °C. The elution solvent was 10% $CH_3CN$ in water at pH 2.0. The elution was carried out in linear gradient mode with a flow rate of 0.5 mL/min. The content of the two sugars was expressed as weight percentage;
- sugar content (°Bx), expressed in Brix degrees, was determined with a manual refractometer (HI 96814, Hanna Instruments); pH was determined by a pH-meter (pH510, XS instruments); titratable acidity (TA), expressed as g/L of tartaric acid, was calculated by titration with 1 M

NaOH solution. Details of the used procedures are reported in the OIV-MA-AS313-01 method [37] and the European official methods [38].

### *2.3 Chemicals*

All solutions were prepared using ultra pure deionised Milli-Q water (18 MΩ/cm resistivity). All chemicals were reagent grade. 3,4-ethylendioxythiophene (EDOT), $LiClO_4$, and anhydrous $CH_3CN$, packaged under nitrogen, were from Sigma-Aldrich. Oenin chloride and (+)-catechin, both of analytical grade, were from Sigma-Aldrich.

### *2.4 Electroanalytical Apparatus and Procedures*

All voltammetric tests were carried out with an Autolab PGSTAT 12 electrochemical instrument (Ecochemie), exploiting computerised control of potential waveform generation and of data acquisition, through GPES dedicated software. The experiments were performed in a single-compartment three-electrode cell, at room temperature, under Ar atmosphere, in order to minimise the presence of interfering oxygen in the solution. A glassy carbon rod served as auxiliary electrode and an aqueous Ag/AgCl, KCl 3M electrode (Metrohm) was the reference electrode. All the potential values given are referred to such an electrode.

The PEDOT-electrode was prepared by direct electrochemical polymerization–deposition onto a 3 mm diameter Pt disk electrode (Metrohm), carried out in a solution containing 10 mM EDOT and 0.1 M $LiClO_4$ supporting electrolyte, $CH_3CN$ de-aerated solvent. Electropolymerisation was performed by the potentiostatic method. A potential of +1.20 V was applied until a charge of 3 mC was spent; the procedure was then terminated by fixing the potential at −0.80 V for 30 s, inducing partial de-doping of the coating. The polymer film was renewed before analysing each sample. Before each electrochemical deposition of PEDOT, the surface of the working electrode was polished with 0.05 μm alumina powder to a mirror finish, dipped in an ultrasonic bath for 10 min, and then rinsed with doubly distilled water.

The SNGC-electrode was prepared as reported in ref. 22. After performing measurements in each sample, the electrode was polished with emery paper (1200 mesh), gently wiped with filtering paper and thoroughly washed with deionized water.

The electrochemical area of the electrodes, determined performing cyclic voltammetry at different scan rates in a 0.5 mM ferrocenedimethanol, 0.1 M KCl aqueous solutions, resulted equal to 0.0753 $cm^2$ (s= 0.004 $cm^2$; n=3) for PEDOT-electrode and to 0.009 $cm^2$ (s= 0.001 $cm^2$; n=4) for SNGC-electrode.

The measurements in the musts samples have been performed without any sample pretreatment, by DPV technique. The DPV waveform consisted of 10 mV potential impulse, 4 mV potential step, 0.15 s impulse time, and 0.6 s time interval between two subsequent potential pulses. Ten subsequent DPV scans were performed in the potential range -0.30 ÷ +0.70 V when using PEDOT-electrode and in the potential range −0.10 ÷ +1.00 V when using SNGC-electrode. Before each scan, the electrode was kept at -0.30 V for 30 seconds (PEDOT-electrode) and at -0.5 V for 120 s (SNGC-electrode). Since polyphenolic substances give rise to pre-concentration phenomena on the electrode surfaces, to an extent resulting a function of the contact time between the electrode and the solution [39], the DPV measurements were started as soon as the electrodes were immersed in the must samples.

For each measured sample, the corresponding voltammetric signal that was further elaborated by multivariate techniques was obtained by merging in sequence the vectors of the current values recorded in the ten subsequent DPV scans, as described in ref. [16]. Each resulting electrochemical signal is considered as a sort of fingerprint of the analysed sample, supposed to bring the chemical information useful for the quantification of the physicochemical parameters related to technological and phenolic maturity.

The rationale for this approach is based on the observation that, although repeatability is not achieved within the set of 10 scans of a single DPV measurement, the reproducibility exhibited by two sets of DPV measurements, each one consisting of ten scans, in the same must with nominally the same electrode, was quite satisfactory, once proper experimental conditions were adopted. The evolution of the electrochemical response within subsequent DPV scans may be reasonably ascribed to two different factors: i) modifications of the electrode surface due to the electroactive species; ii) any other chemical and physical effects on the charge transfer, due to the food matrix. Based on preliminary analyses, ten scans were enough to give exhaustive account of the evolution of the signal due to these effects. As some of us observed in previous articles [16 -19], both the shape and the scan-by-scan evolution of the voltammetric traces are actually informative with respect to discrimination and calibration purposes and, in some cases, not all the ten successive DPV scans contribute to an equal extent. This latter consideration justified the use of iPLS as a feature selection method to improve the performance of the calibration models.

### 2.5 Multivariate data analysis

#### 2.5.1 Exploratory data analysis

Before calculating the calibration models, the three datasets, corresponding to the physico-chemical parameters, to the PEDOT-electrode signals, and to the SNGC-electrode signals, were explored by Principal Component Analysis (PCA) in order to analyse their structure and to detect possible outliers. The matrix of the physico-chemical data, with size equal to {90 samples × 18 parameters}, was preprocessed by autoscaling. The DPV data matrices with size equal to {90 signals × 2430 potential values} and to {90 signals × 2680 potential values} for PEDOT-electrode and SNGC-electrode, respectively, were preprocessed by first order derivative (Savitzky–Golay filtering algorithm with a 15 points filter width, 2$^{nd}$ order polynomial) followed by meancentering. This signal preprocessing method was chosen based on the good results obtained in previous researches on similar food matrices [18,19], and was also used in the following calibration steps.

#### 2.5.2 PLS and iPLS calibration models on the two separate sensors

Firstly, the multivariate calibration models were calculated for each physico-chemical parameter by considering separately from each other the two DPV data matrices corresponding to the PEDOT-electrode and to the SNGC-electrode signals. After a preliminary assessment by PLS of the predictive performance of the models calculated considering the whole DPV data matrix, a selection of the scans leading to the optimal predictive performance was performed by means of iPLS [27].

The performance of the obtained calibration models was expressed in terms of the coefficient of determination, $R^2$ [40-42], calculated in calibration ($R^2_{Cal}$), in cross-validation ($R^2_{CV}$), and in prediction ($R^2_{Pred}$). $R^2$ is particularly useful to compare directly models calculated on different response variables, since it does not depend on the scale of the dependent variable, *y*, and is defined by the following equation:

$$R^2 = 1\text{-}PRESS/SS_y \qquad \text{(eq. 1)}$$

where PRESS is the Prediction Error Sum of Squares, defined as the sum of the squared differences between the experimental and the predicted *y* values, while $SS_y$ is the sum of squares of the experimental *y* values (of the training set for $R^2_{Cal}$ and for $R^2_{CV}$, and of the test set for $R^2_{Pred}$). Essentially, this parameter represents the portion of the variance in the response variable that is

predictable from the calibration model. While $R^2_{Cal}$ corresponds to the squared value of the Pearson correlation coefficient ($r$) between the experimentally measured $y$ values and the corresponding values calculated by the calibration model, resulting necessarily higher than 0, this does not hold for the $R^2_{CV}$ and $R^2_{Pred}$ parameters, which can also assume negative values in case of very bad model performance.
Furthermore, also the values of the Root Mean Square Error (RMSE) [43], calculated in calibration (RMSEC), in cross-validation (RMSECV), and in prediction (RMSEP), were considered. RMSE represents the sample standard deviation of the differences between measured and predicted values, expressed in the same measurement units of the considered dependent variable, and is defined by the following equation:

$$\mathrm{RMSE}=\sqrt{\frac{\mathrm{PRESS}}{n}} \qquad \text{(eq. 2)}$$

where $n$ is the number of samples of the training set (for RMSEC and RMSECV) or of the test set (for RMSEP).

For validation purposes, both the datasets of the signals relative to the two electrode systems were split into a training set, corresponding to the 60 signals recorded on the samples belonging to two field replicates, and into a test set, corresponding to the 30 signals measured on the samples belonging to the remaining field replicates.
The model dimensionality was chosen by minimizing the value of the Root Mean Square Error in Cross-Validation (RMSECV). A venetian blinds cross-validation scheme with 2 deletion groups was considered, where each deletion group contained all the signals acquired on the same field replicate.
Since for each sample 10 DPV scans were acquired in sequence, making the whole signal redundant, iPLS variable selection method was applied to each DPV data matrix in the *forward* mode [44]. Briefly, the *forward* iPLS algorithm divides the signal into a user-defined number of intervals of equal width, then it selects the intervals most useful for calibration by iteratively adding one interval at a time until a significant decrease of RMSECV is no longer observed. An interval width equal to a single DPV scan was chosen, corresponding to 243 points for the PEDOT-electrode dataset and to 268 points for the SNGC-electrode dataset. The same validation scheme used to calculate the PLS models was also applied to the iPLS models.

### *2.5.3 Data fusion*

For each physico-chemical parameter, a final calibration model was calculated by data fusion of the PEDOT-electrode and SNGC-electrode voltammetric data that were previously selected by iPLS. Since the two voltammetric sensors consist of different materials, operate in different potential ranges, and give different responses both in terms of the measured current values and as to the shape of the relevant signals, they could bring different information. For this reason, we have merged the complementary information obtained from these different sensors to produce more consistent, accurate, and useful information than that provided by the two separate data sources, thanks to possible complementarity of the responses of the two electrode systems.

In particular, mid-level data fusion strategy was adopted [28-30], which consisted in combining the features that were previously extracted from each block separately. In general, the extracted features can consist either in the original variables selected from the dataset or in the latent variables obtained by using, for instance, PCA or PLS. In this particular case, the mid-level data fusion was performed by merging together the DPVs selected on the two sets of signals (PEDOT and SNGC) by iPLS for each dependent variable [45], i.e., for each physico-chemical parameter.

Before performing data fusion, the two sets of signals were preprocessed by first order derivative, as for the previous models. Furthermore, given that the measured current values and the number of selected variables was different for the two sensors, to obtain better compatibility before data fusion the data were further preprocessed considering two different methods: block-scaling, which consists in meancentering and then scaling to unit variance each one of the two PEDOT and SNGC blocks, and autoscaling. Conversely to autoscaling, where the same weight is given to each variable, the purpose of block-scaling is to ascribe equal weight to each one of the two PEDOT and SNGC blocks, regardless of the measured current values and of the number of variables contained within each single block.

External validation and cross-validation were performed using the same criteria adopted for the PLS and iPLS models described in the previous paragraph.

All the models presented in this work were calculated using the PLS_Toolbox (ver. 7.8.2, Eigenvector Research Inc.) running in the Matlab environment (ver. 7.12, The Mathworks Inc.).

## 3. Results and discussion

### *3.1 Exploratory analysis of physico-chemical data*

In order to obtain a preliminary overview of the analysed must samples, a PCA model was calculated on the dataset of the physico-chemical parameters listed in section 2.2. Two principal components were selected, accounting for more than 77% of the total data variance. Figure 1 reports the PC1-PC2 biplot, which essentially consists in the superimposition of the corresponding score plot and loading plot. From this figure, it is clear that the three grape varieties (*Ancellotta*, A, *Lambrusco Marani*, L, and *Malbo Gentile*, M) follow a common trend during ripening, mainly from negative to positive values of PC1. The analysis of the variables suggests that, in general, grapes become progressively richer in sugars and anthocyanins, while the acidity decreases with time, as expected. Focusing the attention on the different grape varieties, interestingly they show some peculiar features. In particular, a relatively limited increase of the content of polyphenols, flavonoids and anthocyanins is observed during ripening of M, while for A and L these compounds show a sharp increase starting from T2.

**Figure 1 near here**

*3.2 Exploratory analysis of PEDOT-electrode responses*

Figure 2 reports the voltammetric responses of PEDOT-electrode in musts of the three varieties of grapes at two different ripening levels. For the sake of simplicity, only the 1$^{st}$ scans are shown. It is worth noticing that responses quite different from one another are recorded on the same must at different ripening stages. This suggests that the DPV responses bring useful information with respect to the progress of such a process. Considering that in the voltammetric range investigated PEDOT film undergoes p-doping, it is not surprising that the "background" density current is of ca. 30 μA x cm$^{-2}$.

**Figure 2 near here**

In all the DPV scans two peaks, located at ca. +0.15 V and at ca. +0.45 V (see Figure 2A), are well evident. In some musts or ripening time a third peak at higher potential is also recorded (see Figure 2B). More positive potentials were not investigated, in order to avoid possible overoxidation of the polymer film. In accordance to the literature regarding wines and other beverages rich of polyphenolic substances [46], the presence of two or three anodic peaks in the voltammograms are reasonably

attributable to the oxidation of the cathecol, gallate, phenolic, and methoxy groups of tannins and anthocyanins.

The variations of the features of the DPV curves reported in Figure 2A and 2B, should be principally ascribed to the variation of the concentration and nature of the redox-active species during maturation. Nevertheless, other phenomena, such as the variation of viscosity of the solution, due to the increase of the content of sugars, can be invoked to partly explain the modifications of the electrochemical response (think at the previously discussed matrix effects). Unluckily, sugars are not directly electrochemically detectable in the conditions adopted in this study. Preliminary experiments have been performed in our laboratory in order to explain the effect of sugars content on the voltammetric response. Increasing amounts of sugars were added to a synthetic must solution (300 ppm of oenocyanin in tartrate buffer, pH=3.0) up to final concentrations equal to 10, 15 and 20% w/v. The peak current due to oxidation of the polyphenolic substances progressively decreased in intensity at increasing sugars content. Similar trends arose from an inspection of the voltammetric curves collected for each grape variety at different ripening stages. Nevertheless, the overall modification of the chemical composition of the grapes during ripeness, i.e. variation of sugars and polyphenolic contents, does not allow a simple interpretation of the voltammetric changes of the signals with time.

Figure 3 reports an example of the evolution of the voltammetric signal, changing in intensity and shape, detectable over 10 subsequent potential scans recorded by following the described procedure.

**Figure 3 near here**

As we observed in previous articles [17-19], the scan-after-scan evolution of the voltammetric traces can bring useful information. A most important source of changes in the shapes of voltammograms over subsequent scans lies in adsorption on the electrode surface either of the polyphenolic substances present in the must samples or of their oxidation products: the evolution of the DPV traces does depend upon the nature of the must itself. Repeatable trends are found in the cases of all the analysed samples, testifying a reproducible effect of the matrix on the electrode processes.

For exploratory data analysis purposes, PCA was performed on the electrochemical signals recorded at the PEDOT-electrode, with the aim of evidencing meaningful patterns within the dataset, without making any *a priori* assumption. Interestingly, the distribution of the samples in the PC1-PC3 score plot (Figure 4) partly resembles the structure observed in Figure 1: a common trend for the different varieties of grapes is evidenced, well accounting for the sampling time. The PC1 score values decrease

from T0 to T4, while the PC3 values increase from T0 to T1, and then decrease from T2 to T4. At veraison (T0), in Figure 1, and even more markedly in Figure 4, the M samples show extreme values of PC1.

**Figure 4 near here**

*3.3 Exploratory data analysis on SNGC-electrode responses*

The DPV signals measured with the SNGC-electrode on musts (Figure 5A and 5B) present more peaks and more complex features with respect to the signals recorded using the PEDOT-electrode, also thanks to the possibility to investigate a wider potential region. Interestingly, the DPV traces recorded with the SNGC-electrode at time 4 of maturation (Figure 5B) show an intense peak located at ca. +0.60 V, while in the DPV signals collected with PEDOT-electrode and reported in Figure 2 B the peak at ca. +0.45 V is still the highest one. This could suggest a discriminant behaviour of the two electrodes with respect the different phenolic species present in solution, which are reported in literature to be oxidised at different potentials.

**Figure 5 near here**

In accordance with refs. 47 and 48, all hydroxyl groups of the anthocyanins present in *Vitis vinifera* can be electrochemically oxidized at a carbon electrode, giving rise to several peaks in the DPV signals, as a function of the substituents on the B ring of the flavylium cation.
The evolution of the DPV traces over 10 subsequent DPV scans is similar to that observed using the PEDOT-electrode (Figure 6).

**Figure 6 near here**

PCA performed on the DPV curves acquired with the SNGC-electrode evidences evolution of the signals with ripening, as reported in Figure 7, where the score plot of the first two PCs is represented. PC1 and PC2 account together for ca. 75% of the total variance. Although in this plot the samples are arranged differently than in Figure 1, the three grape varieties follow a common trend, according to the sampling time, highlighted by the blue arrow. This indicates that the electrochemical signals bring

information related to chemical changes occurring during grape ripening, which is better investigated through the development of calibration models that include all the considered varieties, as reported hereafter.

**Figure 7 near here**

### *3.4 Calibration of physico-chemical parameters*

Based on the encouraging results obtained from the exploratory data analysis of the three datasets, the electrochemical signals recorded with both the electrodes have been used to build multivariate calibration models, in order to evaluate the capability to predict the values of the considered physico-chemical parameters.

As described in the previous sections, the first step consisted in the definition, for each voltammetric sensor, of PLS models based on the whole sequences of the voltammetric curves. The prediction results of each physico-chemical parameter are reported in Table 1, together with the indication of the model dimensionality, i.e. of the number of latent variables (#LVs) used.

| PEDOT-electrode | | | | | | | |
|---|---|---|---|---|---|---|---|
| **Y variable** | **#LVs** | **RMSEC** | **RMSECV** | **RMSEP** | **$R^2_{Cal}$** | **$R^2_{CV}$** | **$R^2_{Pred}$** |
| **TF (mg/L)** | 4 | 27.22 | 33.80 | 29.85 | 0.70 | 0.54 | 0.54 |
| **TAnt (mg/L)** | 4 | 41.35 | 48.34 | 40.64 | 0.78 | 0.69 | 0.78 |
| **Ton** | 3 | 0.18 | 0.19 | 0.21 | 0.81 | 0.78 | 0.66 |
| **CI** | 4 | 1.64 | 2.03 | 1.61 | 0.77 | 0.64 | 0.78 |
| **OD420%** | 4 | 4.19 | 5.27 | 6.13 | 0.88 | 0.81 | 0.73 |
| **OD520%** | 3 | 5.78 | 6.57 | 7.36 | 0.82 | 0.77 | 0.66 |
| **OD620%** | 1 | 1.92 | 2.07 | 1.90 | 0.25 | 0.13 | -1.09 |
| **TP (mg/L)** | 1 | 1500.90 | 1687.30 | 1629.20 | 0.09 | -0.15 | -0.12 |
| **Df-3-glc (mg/L)** | 5 | 4.13 | 4.97 | 10.55 | 0.69 | 0.55 | 0.37 |
| **Cn-3-glc (mg/L)** | 2 | 2.54 | 2.69 | 7.97 | 0.45 | 0.38 | -0.22 |
| **Pt-3-glc (mg/L)** | 5 | 6.42 | 7.99 | 9.34 | 0.72 | 0.57 | 0.59 |
| **Pn-3-glc (mg/L)** | 2 | 7.90 | 8.31 | 14.75 | 0.54 | 0.49 | 0.17 |
| **Mv-3-glc (mg/L)** | 4 | 33.72 | 40.60 | 36.76 | 0.85 | 0.78 | 0.76 |
| **°Bx** | 3 | 2.08 | 2.27 | 2.88 | 0.73 | 0.69 | 0.57 |
| **Glu (%)** | 3 | 1.44 | 1.57 | 2.22 | 0.77 | 0.73 | 0.65 |
| **Fru (%)** | 3 | 1.20 | 1.31 | 1.90 | 0.81 | 0.78 | 0.68 |
| **pH** | 5 | 0.21 | 0.26 | 0.19 | 0.75 | 0.60 | 0.83 |
| **TA (meq/L)** | 2 | 17.42 | 17.31 | 19.70 | 0.93 | 0.93 | 0.93 |
| **SNGC-electrode** | | | | | | | |
| **Y variable** | **#LVs** | **RMSEC** | **RMSECV** | **RMSEP** | **$R^2_{Cal}$** | **$R^2_{CV}$** | **$R^2_{Pred}$** |
| **TF (mg/L)** | 5 | 23.99 | 32.30 | 26.75 | 0.77 | 0.58 | 0.63 |
| **TAnt (mg/L)** | 5 | 39.58 | 55.79 | 42.83 | 0.79 | 0.59 | 0.76 |

| | | | | | | | |
|---|---|---|---|---|---|---|---|
| **Ton** | 5 | 0.16 | 0.22 | 0.16 | 0.83 | 0.69 | 0.81 |
| **CI** | 5 | 1.66 | 2.42 | 1.75 | 0.76 | 0.49 | 0.74 |
| **OD420%** | 5 | 4.54 | 6.21 | 4.45 | 0.86 | 0.73 | 0.86 |
| **OD520%** | 5 | 5.70 | 7.64 | 5.64 | 0.83 | 0.69 | 0.80 |
| **OD620%** | 1 | 1.97 | 2.22 | 1.95 | 0.21 | 0.00 | -1.20 |
| **TP (mg/L)** | 3 | 1168.20 | 1453.00 | 1225.30 | 0.45 | 0.14 | 0.36 |
| **Df-3-glc (mg/L)** | 4 | 4.47 | 5.31 | 10.21 | 0.63 | 0.49 | 0.41 |
| **Cn-3-glc (mg/L)** | 4 | 2.13 | 2.43 | 6.70 | 0.61 | 0.49 | 0.13 |
| **Pt-3-glc (mg/L)** | 5 | 5.98 | 7.79 | 8.18 | 0.76 | 0.60 | 0.69 |
| **Pn-3-glc (mg/L)** | 5 | 6.47 | 10.08 | 9.76 | 0.69 | 0.25 | 0.64 |
| **Mv-3-glc (mg/L)** | 5 | 30.06 | 39.26 | 28.26 | 0.88 | 0.80 | 0.86 |
| **°Bx** | 2 | 2.68 | 2.94 | 2.78 | 0.56 | 0.47 | 0.60 |
| **Glu (%)** | 2 | 2.01 | 2.13 | 2.52 | 0.56 | 0.51 | 0.55 |
| **Fru (%)** | 3 | 1.56 | 1.86 | 2.00 | 0.68 | 0.55 | 0.64 |
| **pH** | 5 | 0.18 | 0.25 | 0.34 | 0.80 | 0.62 | 0.47 |
| **TA (meq/L)** | 5 | 21.01 | 26.79 | 36.86 | 0.90 | 0.84 | 0.77 |

**Table 1:** Calibration results from PLS models for the investigated properties, using the two different electrodes.

Considering the results in prediction, the PEDOT-electrode shows the most satisfactory performance for the prediction of CI, pH, TA and TAnt. Among the single anthocyanins, a satisfactory performance has been obtained for the prediction of malvidine-3-O-glucoside ($R^2_{Pred}$ = 0.76). Quite unexpectedly, the PEDOT-electrode shows acceptable results also in the prediction of the parameters related to the sugar content (°Bx, Glu and Fru). In fact, sugars are not oxidisable in the experimental conditions adopted in this study. Therefore, an indirect effect of the variation of the sugars content during ripening of grapes on the electrochemical response should be invoked: the matrix effect does contribute to the total content of useful information.

As far as the SNGC-electrode is concerned, the relevant PLS model leads to satisfactory prediction models for TAnt, Ton, CI, OD420% and OD520%, Mv-3-glc and TA. Compared to PEDOT-electrode, SNGC-electrode leads in general to better results in the prediction of the five most abundant anthocyanins and of the parameters derived by the UV-Vis measurements. It must be highlighted that with both the voltammetric sensors it was not possible to obtain an estimate of OD620%. This fact is reasonably ascribable to the very low values of absorbance at 620 nm, scarcely distinguishable from those of the baseline.

Variable selection through iPLS was then applied separately to the two datasets of electrochemical signals, with the aim of selecting the combinations of DPV scans leading to the best calibration models

for each physico-chemical parameter. The results of the iPLS models are reported in Table 2, where the second column reports the numbers corresponding to the selected DPV scans.

With respect to the PLS results reported in Table 1, the variable selection generally leads to slight improvements of the models performance, as reported in Table 2. The improvement is more pronounced for the PEDOT-electrode, in particular as to the variables accounting for the sugar content, which in this case are predicted quite satisfactorily. With regard to the number of selected variables, the models built up with the responses of the PEDOT-electrode are often more parsimonious than in the case of the SNGC-electrode. Scans n. 1, 2, and 7 were the most frequently selected ones for the SNGC-electrode, while for the PEDOT-electrode the major part of the models included scans n. 10 and 3. These results confirm the advantage of considering the variation of the response of the voltammetric sensors between the different scans, which is due to interactions between electrode and grape must.

| PEDOT-electrode | | | | | | | | |
|---|---|---|---|---|---|---|---|---|
| **Y variable** | **sel. DPV scan #** | **#LVs** | **RMSEC** | **RMSECV** | **RMSEP** | **$R^2_{Cal}$** | **$R^2_{CV}$** | **$R^2_{Pred}$** |
| **TF (mg/L)** | 3, 10 | 4 | 27.24 | 32.41 | 27.80 | 0.70 | 0.57 | 0.60 |
| **TAnt (mg/L)** | 3 | 4 | 41.57 | 46.38 | 37.20 | 0.77 | 0.72 | 0.82 |
| **Ton** | 9 | 3 | 0.17 | 0.18 | 0.21 | 0.82 | 0.80 | 0.67 |
| **CI** | 2, 3 | 4 | 1.74 | 1.93 | 1.40 | 0.74 | 0.68 | 0.83 |
| **OD420%** | 10 | 5 | 3.92 | 4.72 | 5.72 | 0.89 | 0.85 | 0.77 |
| **OD520%** | 10 | 5 | 5.08 | 5.91 | 7.40 | 0.86 | 0.81 | 0.66 |
| **OD620%** | 2 | 1 | 1.92 | 2.04 | 1.93 | 0.25 | 0.15 | -1.15 |
| **TP (mg/L)** | 4 | 1 | 1498.60 | 1681.40 | 1635.50 | 0.09 | -0.15 | -0.13 |
| **Df-3-glc (mg/L)** | 1, 3, 6, 9 | 5 | 4.09 | 4.63 | 10.30 | 0.69 | 0.61 | 0.40 |
| **Cn-3-glc (mg/L)** | 10 | 4 | 2.19 | 2.60 | 7.62 | 0.59 | 0.42 | -0.12 |
| **Pt-3-glc (mg/L)** | 1, 3 | 5 | 6.16 | 6.89 | 8.65 | 0.75 | 0.68 | 0.65 |
| **Pn-3-glc (mg/L)** | 3 | 2 | 7.80 | 8.19 | 14.66 | 0.55 | 0.50 | 0.18 |
| **Mv-3-glc (mg/L)** | 3, 4, 6, 10 | 5 | 27.80 | 37.40 | 29.90 | 0.90 | 0.81 | 0.84 |
| **°Bx** | 10 | 5 | 1.83 | 2.12 | 1.99 | 0.80 | 0.72 | 0.79 |
| **Glu (%)** | 10 | 5 | 1.33 | 1.55 | 1.74 | 0.81 | 0.74 | 0.79 |
| **Fru (%)** | 10 | 5 | 1.09 | 1.26 | 1.47 | 0.85 | 0.79 | 0.81 |
| **pH** | 1, 10 | 3 | 0.23 | 0.25 | 0.20 | 0.68 | 0.63 | 0.82 |
| **TA (meq/L)** | 8, 10 | 2 | 16.73 | 17.23 | 18.63 | 0.94 | 0.94 | 0.94 |
| **SNGC-electrode** | | | | | | | | |
| **Y variable** | **sel. DPV scan #** | **#LVs** | **RMSEC** | **RMSECV** | **RMSEP** | **$R^2_{Cal}$** | **$R^2_{CV}$** | **$R^2_{Pred}$** |
| **TF (mg/L)** | 1, 6, 7 | 5 | 23.16 | 30.84 | 25.69 | 0.78 | 0.61 | 0.66 |
| **TAnt (mg/L)** | 6 | 5 | 40.71 | 55.80 | 48.51 | 0.78 | 0.59 | 0.69 |
| **Ton** | 1, 4, 5 | 5 | 0.16 | 0.21 | 0.16 | 0.84 | 0.73 | 0.81 |
| **CI** | 1, 2, 10 | 4 | 1.87 | 2.29 | 2.02 | 0.70 | 0.55 | 0.65 |
| **OD420%** | 8 | 4 | 5.75 | 6.42 | 5.68 | 0.77 | 0.72 | 0.77 |
| **OD520%** | 1, 4, 5, 8 | 5 | 5.62 | 7.26 | 5.48 | 0.83 | 0.72 | 0.81 |
| **OD620%** | 1, 2 | 1 | 1.94 | 2.19 | 1.90 | 0.24 | 0.03 | -1.07 |

| | | | | | | | | |
|---|---|---|---|---|---|---|---|---|
| **TP (mg/L)** | 1 | 3 | 1153.50 | 1362.70 | 1228.80 | 0.46 | 0.25 | 0.36 |
| **Df-3-glc (mg/L)** | 2, 7, 8, 10 | 5 | 3.95 | 5.27 | 9.52 | 0.71 | 0.49 | 0.49 |
| **Cn-3-glc (mg/L)** | 2, 6 | 5 | 1.97 | 2.39 | 6.54 | 0.67 | 0.51 | 0.18 |
| **Pt-3-glc (mg/L)** | 2, 8, 10 | 5 | 5.74 | 7.69 | 7.84 | 0.78 | 0.61 | 0.71 |
| **Pn-3-glc (mg/L)** | 1, 2, 3 | 4 | 6.90 | 9.48 | 10.93 | 0.65 | 0.33 | 0.54 |
| **Mv-3-glc (mg/L)** | 2, 7, 10 | 5 | 30.57 | 39.59 | 30.61 | 0.88 | 0.79 | 0.83 |
| **°Bx** | 7, 9 | 3 | 2.59 | 2.93 | 2.67 | 0.59 | 0.48 | 0.63 |
| **Glu (%)** | 7, 10 | 3 | 1.86 | 2.07 | 2.29 | 0.62 | 0.54 | 0.63 |
| **Fru (%)** | 7, 10 | 3 | 1.62 | 1.78 | 1.93 | 0.66 | 0.59 | 0.67 |
| **pH** | 1, 6, 7, 8, 9 | 5 | 0.18 | 0.24 | 0.34 | 0.81 | 0.66 | 0.46 |
| **TA (meq/L)** | 2, 9 | 5 | 22.73 | 27.46 | 38.91 | 0.89 | 0.84 | 0.74 |

**Table 2:** Calibration results after iPLS variable selection obtained for both the PEDOT-electrode signals (above) and the SNGC-electrode signals (below).

The comparison of the calibration models reported in Table 1 and in Table 2 shows that the two voltammetric sensors bear different information from each other. For example, the results reported in Table 2 show that PEDOT-electrode leads to much better results than SNGC-electrode for the prediction of TA, while the opposite is observed, e.g., for OD520%. These results confirmed that the two voltammetric sensors actually bear different pieces of information about the investigated food matrix. It follows that data fusion could allow to acquire more information content, thanks to the possible complementarity of the PEDOT and SNGC responses.

For each physico-chemical property, data fusion was therefore accomplished by merging in sequence the DPV scans selected by iPLS for both the electrodes, and calculating PLS models on the resulting signals. As it was described in the experimental section, two different preprocessing methods were applied on the fused data, i.e. autoscaling and block-scaling. The results of the calibration models obtained after data fusion of the selected variables are reported in Table 3, together with the total number of variables used to build the corresponding model (# sel vars).

The comparison of the data in Table 3 with those in Tables 1 and 2 evidences that the adoption of the fused models leads to the achievement of a general improvement of the predictive performance, even if for some parameters the single-electrode models work actually better. In general, considering the 15 parameters for which acceptable performance in prediction ($R^2_{Pred}$ >0.5) is obtained at least for one of the calculated models, in eight cases the best performance is obtained considering the fused data, while in one case data fusion leads to the same performance obtained by considering a single electrode.

More in detail, for TF, TAnt and CI, data fusion and autoscaling pretreatment leads to intermediate $R^2_{Pred}$ values, compared to those obtained from the iPLS models of the individual electrodes. For

instance, for CI, $R^2_{Pred}$ values equal to 0.83, 0.65, and 0.74 have been obtained with the PEDOT-electrode model, with the SNGC-electrode model and with the fused data model, respectively. Concerning the models on fused data preprocessed by block-scaling, significant improvements are achieved for the prediction of Ton, OD520% and Mv-3-glc. Satisfactory results are obtained for the parameters referred to the sugar content (Glu, Fru and °Bx) and for pH; for these parameters the models built on the fused data perform better than the corresponding models built on the single-electrode signals. Among all the considered parameters, the best performance in prediction is gained for TA, for which a value of $R^2_{Pred}$ equal to 0.94 was obtained both with iPLS on PEDOT-electrode signals and with the two models on fused data.

Finally, it must be highlighted that data fusion generally leads to a decrease of the number of latent variables, with respect to the corresponding models calculated for the individual electrodes.

Summarizing, in most cases data fusion allows to enhance the information individually carried by the two single electrodes for the quantitative determination of a significant number of parameters of interest. These results lay the foundations for the development of an electronic tongue for actual in field applications.

| Selected variables fusion (autoscaling) | | | | | | | | |
|---|---|---|---|---|---|---|---|---|
| **Y variable** | **# sel vars** | **#LVs** | **RMSEC** | **RMSECV** | **RMSEP** | **$R^2_{Cal}$** | **$R^2_{CV}$** | **$R^2_{Pred}$** |
| **TF (mg/L)** | 1290 | 3 | 24.55 | 30.79 | 31.84 | 0.76 | 0.64 | 0.63 |
| **TAnt (mg/L)** | 511 | 2 | 43.58 | 49.97 | 46.60 | 0.75 | 0.67 | 0.74 |
| **Ton** | 1047 | 2 | 0.17 | 0.19 | 0.18 | 0.81 | 0.77 | 0.78 |
| **CI** | 1290 | 2 | 1.77 | 2.06 | 1.79 | 0.73 | 0.64 | 0.74 |
| **OD420%** | 511 | 2 | 4.05 | 4.45 | 6.38 | 0.89 | 0.86 | 0.79 |
| **OD520%** | 1315 | 2 | 5.72 | 6.68 | 6.49 | 0.83 | 0.77 | 0.77 |
| **OD620%** | 779 | 1 | 1.77 | 2.05 | 2.00 | 0.36 | 0.20 | 0.08 |
| **TP (mg/L)** | 511 | 1 | 1341.71 | 1591.32 | 1397.44 | 0.27 | 0.08 | 0.35 |
| **Df-3-glc (mg/L)** | 511 | 5 | 3.57 | 4.87 | 10.57 | 0.77 | 0.60 | 0.45 |
| **Cn-3-glc (mg/L)** | 779 | 3 | 2.02 | 2.42 | 6.95 | 0.65 | 0.51 | 0.39 |
| **Pt-3-glc (mg/L)** | 1290 | 3 | 5.92 | 7.20 | 9.14 | 0.77 | 0.66 | 0.63 |
| **Pn-3-glc (mg/L)** | 1047 | 1 | 8.37 | 9.15 | 12.10 | 0.48 | 0.39 | 0.52 |
| **Mv-3-glc (mg/L)** | 1776 | 5 | 22.12 | 33.46 | 30.94 | 0.94 | 0.86 | 0.88 |
| **°Bx** | 779 | 2 | 2.08 | 2.30 | 2.19 | 0.74 | 0.68 | 0.85 |
| **Glu (%)** | 779 | 4 | 1.19 | 1.52 | 1.68 | 0.85 | 0.76 | 0.84 |
| **Fru (%)** | 779 | 4 | 1.00 | 1.26 | 1.52 | 0.87 | 0.80 | 0.85 |
| **pH** | 1826 | 4 | 0.18 | 0.21 | 0.22 | 0.81 | 0.74 | 0.86 |
| **TA (meq/L)** | 1022 | 2 | 16.51 | 20.60 | 23.50 | 0.94 | 0.91 | 0.94 |
| **Selected variables fusion (block-scaling)** | | | | | | | | |
| **Y variable** | **# sel vars** | **#LVs** | **RMSEC** | **RMSECV** | **RMSEP** | **$R^2_{Cal}$** | **$R^2_{CV}$** | **$R^2_{Pred}$** |
| **TF (mg/L)** | 1290 | 4 | 24.23 | 28.23 | 35.09 | 0.76 | 0.68 | 0.56 |
| **TAnt (mg/L)** | 511 | 2 | 52.30 | 54.35 | 62.07 | 0.64 | 0.61 | 0.56 |
| **Ton** | 1047 | 5 | 0.12 | 0.17 | 0.16 | 0.91 | 0.84 | 0.88 |

| | | | | | | | | |
|---|---|---|---|---|---|---|---|---|
| **CI** | 1290 | 3 | 1.71 | 2.05 | 2.09 | 0.75 | 0.64 | 0.67 |
| **OD420%** | 511 | 3 | 4.58 | 4.96 | 6.20 | 0.86 | 0.83 | 0.83 |
| **OD520%** | 1315 | 5 | 4.00 | 6.26 | 5.15 | 0.91 | 0.81 | 0.87 |
| **OD620%** | 779 | 1 | 1.90 | 2.06 | 1.84 | 0.27 | 0.16 | 0.10 |
| **TP (mg/L)** | 511 | 3 | 1127.56 | 1541.27 | 1234.54 | 0.48 | 0.13 | 0.53 |
| **Df-3-glc (mg/L)** | 511 | 4 | 4.46 | 5.34 | 10.59 | 0.64 | 0.49 | 0.41 |
| **Cn-3-glc (mg/L)** | 779 | 4 | 1.92 | 2.28 | 6.82 | 0.68 | 0.56 | 0.40 |
| **Pt-3-glc (mg/L)** | 1290 | 4 | 6.55 | 8.08 | 9.48 | 0.71 | 0.57 | 0.60 |
| **Pn-3-glc (mg/L)** | 1047 | 4 | 5.68 | 8.14 | 10.85 | 0.76 | 0.56 | 0.61 |
| **Mv-3-glc (mg/L)** | 1776 | 5 | 26.45 | 38.38 | 29.20 | 0.91 | 0.81 | 0.89 |
| **°Bx** | 779 | 3 | 1.90 | 2.12 | 2.34 | 0.78 | 0.73 | 0.85 |
| **Glu (%)** | 779 | 3 | 1.31 | 1.49 | 1.83 | 0.82 | 0.76 | 0.81 |
| **Fru (%)** | 779 | 3 | 1.08 | 1.27 | 1.62 | 0.85 | 0.79 | 0.83 |
| **pH** | 1826 | 5 | 0.17 | 0.21 | 0.22 | 0.82 | 0.74 | 0.85 |
| **TA (meq/L)** | 1022 | 2 | 16.59 | 18.25 | 22.51 | 0.94 | 0.93 | 0.94 |

**Table 3:** PLS results obtained after data fusion of the selected variables preprocessed using autoscaling (above) and block-scaling (below).

## Conclusions

The potential usefulness of an ET consisting of PEDOT- and SNGC-electrodes in monitoring the grape ripening process has been investigated. The adopted procedure consisted in analysing responses from DPV measurements, performed directly in the must, without the necessity to add any reagents. Data fusion allowed to condense the information brought by the two electrodes for the quantitative determination of a number of parameters of interest in the estimation of the ripening of the grapes, such as pH, total acidity, sugar contents and tonality.

These results allowed to develop an effective two-sensor voltammetric ET sensing system for direct application in grape must. On the whole, the ET sensing system allows to obtain very satisfactory results ($R^2_{Pred}$ values from 0.82 to 0.94) for 11 out of the 18 physicochemical parameters that were considered in this work, and at least an acceptable estimate was reached ($R^2_{Pred}$ values from 0.53 to 0.71) for further 4 parameters.

Additional tests are in progress in our laboratory using commercially available, disposable PEDOT-electrodes. The definition of an effective methodology for similar electrode systems would allow the polymerisation step to be avoided, making the measurements faster and more practical.

Finally, further work is in progress on the same samples in our labs, devoted to the development of an EE sensing system for the prediction of colour-related parameters suitable to monitor the ripening of grape.

**Acknowledgements**

The authors acknowledge financial support for this research by University of Modena and Reggio Emilia through FAR 2014. The Authors are grateful to "Istituto Superiore A. Zanelli", Reggio Emilia – Italy, for providing grape samples.

**Conflict of interest**

The authors declare that they have no conflict of interest.

**References**

1. P. Butz, C. Hofmann, B. Tauscher, Recent developments in noninvasive techniques for fresh fruit and vegetable internal quality analysis, J. Food Sci. 70 (2005) R131-R141.
2. H. Huang, H. Yu, H. Xu, Y. Ying, Near infrared spectroscopy for on/in-line monitoring of quality in foods and beverages: A review, J. Food Eng. 87 (2008) 303-313
3. A. Loutfi, S. Coradeschi, G.K. Mani, P. Shankar, J.B.B. Rayappan, Electronic noses for food quality: A review, J. Food Eng, 144 (2015) 103-111.
4. J. Gutiérrez, M.C. Horrillo, Advances in artificial olfaction: Sensors and applications, Talanta 124 (2014) 95-105.
5. A. Riul Jr., C.A.R. Dantas, C.M. Miyazaki, O.N. Oliveira Jr., Recent advances in electronic tongues, Analyst, 135 (2010) 2481-2495.
6. L. Escuder-Gilabert, M. Peris, Review: Highlights in recent applications of electronic tongues in food analysis, Anal. Chim. Acta, 665 (2010) 15-25.
7. D. Wu, D.-W. Sun, Colour measurements by computer vision for food quality control - A review, Trends Food Sci. Tech. 29 (2013) 5-20.
8. P. Jackman, D.-W. Sun, Recent advances in image processing using image texture features for food quality assessment, Trends Food Sci. Tech. 29 (2013) 35-43.
9. Q. Ouyang, J. Zhao, Q. Chen, Instrumental intelligent test of food sensory quality as mimic of human panel test combining multiple cross-perception sensors and data fusion, Anal. Chim. Acta 841 (2014) 68-76
10. I. Campos, R. Bataller, R. Armero, J.M. Gandia, J. Soto, R. Martinez-Manez, L. Gil-Sanchez, Monitoring grape ripeness using a voltammetric electronic tongue, Food Reas. Int. 54 (2013) 1369-1375.
11. M. Liu, J. Wang, D. Li, M. Wang, Electronic Tongue Coupled with Physicochemical Analysis for the Recognition of Orange Beverages, J. Food Qual. 35(6) (2012) 429-441.
12. F. Hossein-Babaei, K. Nemati, A concept of microfluidic electronic tongue, Microfluid. Nanofluidics, 13(2) (2012) 331-344.

13. X. Cetó, C. Apetrei, M. Del Valle, M.L. Rodríguez-Méndez, Evaluation of red wines antioxidant capacity by means of a voltammetric e-tongue with an optimized sensor array, Electrochim. Acta 120 (2014) 180-186.
14. M. Scampicchio, D. Ballabio, A. Arecchi, S.M. Cosio, S. Mannino, Amperometric eletronic tongue for food analysis, Microchim. Acta 163 (2008) 11-21.
15. F. Winquist, Voltammetric electronic tongues - Basic principles and applications, Microchim. Acta 163(1-2) (2008) 3-10.
16. V. Martina, K. Ionescu, L. Pigani, F. Terzi, A. Ulrici, C. Zanardi, R. Seeber, Development of an electronic tongue based on a PEDOT-modified voltammetric sensor. Anal. Bioanal. Chem. 387 (2007) 2101-2110.
17. L. Pigani , G. Foca, K. Ionescu, V. Martina, A. Ulrici, F. Terzi, M. Vignali, C. Zanardi, R. Seeber, Amperometric sensors based on poly(3,4-ethylenedioxythiophene)-modified electrodes. Discrimination of white wines, Anal. Chim. Acta, 614 (2008) 213-222.
18. L. Pigani, G. Foca, A. Ulrici, K. Ionescu, V. Martina, F. Terzi, M. Vignali, C. Zanardi, R. Seeber, Classification of red wines by chemometric analysis of voltammetric signals from pedot-modified electrodes,. Anal. Chim. Acta 643 (2009) 67-73.
19. L. Pigani, A. Culetu, A. Ulrici, G. Foca, M. Vignali, R. Seeber, Pedot modified electrodes in amperometric sensing for analysis of red wine samples, Food Chem. 129 (2011) 226-233.
20. M. del Mar Cordero, J.L. Hidalgo, E. Blanco, I. Naranjo, The sonogel-carbon electrodeas a sol-gel graphite-based electrode, Anal. Chem. 74 (2002) 2423-2427.
21. M. del Mar Cordero, I. Naranjo, J.M. Pacios, L. Cubillana, J.L. Hidalgo, Study of the responses of a sonogel-carbon electrode towards phenolic compounds, Electroanal. 17 (2005) 806-814.
22. L.M. Cubillana-Aguilera, J.M. Palacios-Santander, I. Naranjo-Rodríguez, J.L. Hidalgo-Hidalgo-De-Cisneros, Study of the influence of the graphite powder particle size on the structure of the Sonogel-Carbon materials, J. Sol-Gel Sci. Techn. 40 (2006) 55-64.
23. L.F. da Silva, N.R. Stradiotto, H.P. Oliveira, Determination of caffeic acid in red wine by voltammetric Method, Electroanal. 20 (2008) 1252-1258.
24. O. Makhotkina, P.A. Kilmartin, H. Zou, A. Waterhous, The use of cyclic voltammetry for wine analysis: determination of polyphenols and free sulfur dioxide, Anal. Chim. Acta 668 (2010) 155-165.
25. K.H. Hui, A. Ambrosi, M. Pumera, A. Bonanni, Improving the analytical performance of graphene oxide towards the assessment of polyphenols, Chem. Eur. J. 22 (2016) 3830-3834.
26. A. Goowin, C.E. Banks, R.G. Compton, Electroanalytical sensing of green tea anticarcinogenic catechin compounds: epigallicatechin gallate and epigallocatechin, Electroanal. 18 (2006) 849-853.
27. L. Norgaard, A. Saudland, J. Wagner, J.P. Nielsen, L. Munck, S.B. Engelsen, Interval partial least-squares regression (iPLS): A comparative chemometric study with an example from near-infrared spectroscopy. Applied Spectroscopy, 54 (2000) 413–419.
28. E. Acar, M.A. Rasmussen, F. Savorani, T. Næs, R. Bro, Understanding data fusion within the framework of coupled matrix and tensor factorizations. Chemom. Intell. Lab. Syst., 129 (2013) 53–63.

29. B. Khaleghi, A. Khamis, F.O. Karray, S.N. Razavi, Multisensor data fusion: a review of the state-of-the-art. Inform. Fusion. 14 (2013) 28–44.
30. R. Calvini, G. Foca, A. Ulrici, Data dimensionality reduction and data fusion for fast characterization of green coffee samples using hyperspectral sensors. Anal Bioanal Chem 408 (2016) 7351–7366.
31. R. Di Stefano, M.C. Cravero, Metodi per lo studio dei polifenoli dell'uva, Riv. Vitic. Enol. 2 (1991) 37-45.
32. P. Ribéreau-Gayon, Y. Glories, A. Maujean, D. Dubourdieu, Handbook of Enology Volume 2: The Chemistry of Wine Stabilization and Treatments. John Wiley & Sons. New York. 2006. pp 178.
33. Y. Glories, La couleur des vins rouges. Mesure, origine et interprétation. Partie I Connaiss. Vigne Vin. 18 (1984) 195-217.
34. Compendium of international methods of analysis – OIV, Folin-Ciocalteu Index (2015) Available online http://www.oiv.int/public/medias/2477/oiv-ma-as2-10.pdf
35. F. Chinnici, F. Sonni, N. Natali, S. Galassi, C. Riponi, Colour features and pigment composition of Italian carbonic macerated red wines, Food Chem. 113 (2009) 651-657.
36. G. Vasile Simone, G. Montevecchi, F. Masino,V. Matrella S.A. Imazio, A. Antonelli, C. Bignami. Ampelographic and chemical characterization of Reggio Emilia and Modena (northern Italy) grapes for two traditional seasonings: 'saba' and 'agresto', J. Sci. Food Agric. 93 (2013) 3502–3511.
37. Compendium of international methods of analysis – OIV, Total Acidity (2015) Available online http://www.oiv.int/public/medias/3731/oiv-ma-as313-01.pdf
38. EU Official Gazette. L 272, Luxembourg, Oct 3, 33 (1990) Available online http://eur-lex.europa.eu/legal-content/EN/TXT/PDF/?uri=OJ:L:1990:272:FULL&from=IT
39. Q. Zhang, P.A. Kilmartin, Adsorption effects during the analysis of caffeic acid at PEDOT electrodes, Int. J. Nanotech. 14 (2017) 496-504.
40. V. Consonni, D. Ballabio, R. Todeschini, Comments on the Definition of the Q2 Parameter for QSAR Validation, J. Chem. Inf. Model. 49 (2009) 1669–1678.
41. A. Marti, A. Ulrici, G. Foca, L. Quaglia, M.A. Pagani, Characterization of common wheat flours (Triticum aestivum L.) through multivariate analysis of conventional rheological parameters and gluten peak test indices, LWT - Food Sci. Technol., 64 (2015) 95–103.
42. G. Foca, C. Ferrari, A. Ulrici, M.C. Ielo, G. Minelli, D.P. Lo Fiego, Iodine Value and Fatty Acids Determination on Pig Fat Samples by FT-NIR Spectroscopy: Benefits of Variable Selection in the Perspective of Industrial Applications, Food Anal. Meth. 9 (2016), 2791-2806.
43. B.H. Mevik, H.R. Cederkvist, Mean squared error of prediction (MSEP) estimates for principal component regression (PCR) and partial least squares regression (PLSR), J. Chemom. 18 (2004) 422-429.
44. Z. Xiaobo, Z. Jiewen, M.J. Povey, M. Holmes, M. Hanpin, Variables selection methods in near-infrared spectroscopy, Anal. Chim. Acta 667 (2010) 14-32.
45. C. Márquez, M.I. López, I. Ruisánchez, M.P. Callao, FT-Raman and NIR spectroscopy data fusion strategy for multivariate qualitative analysis of food fraud, Talanta 161 (2016) 80-86.

46. H. Karaosmanoglu, W. Suthanthangjai, J. Travas-Sejdic, P.A. Kilmartin, Electyrochemical analysis of beverage phenolics using an electrode modified with poly(3,4-ethylendioxithiophene), Electrochim. Acta 201 (2016) 366-373.
47. P. Janeiro, A.M. Oliveira Brett, Redox behavior of anthocyanins present in Vitis vinifera L., Electroanal. 19 (2007) 1779-1786.
48. M.J. Aguirre, Y.Y. Chen, M. Isaacs, B. Matsuihir, L. Mendoza, A. Torres, Electrochemical behavior and antioxidant capacity of anthocyanins from Chilean red wine, grape and raspberry, Food Chem. 121 (2010) 44-48.

**Captions to Figures**

**Figure 1:** Biplot of the first two PCs obtained from PCA on physicochemical data of must samples.

**Figure 2:** 1st DPV scans recorded by PEDOT-electrode on the three varieties of grapes considered, collected at A) T0 and B) T4.

**Figure 3:** 10 subsequent DPV traces recorded at PEDOT-electrode in an L must, collected at T3.

**Figure 4:** PC1 vs. PC3 score plot for the signals obtained by PEDOT-electrode.

**Figure 5:** 1st DPV scans recorded by SNGC-electrode on the three varieties of grapes collected at A) T0 and B) T4.

**Figure 6:** 10 subsequent DPV scans recorded with SNGC-electrode in an L must, collected at T3.

**Figure 7:** PC1 vs. PC2 score plot for the signals obtained by the SNGC-electrode.

Highlights

- An electronic tongue has been developed aiming at monitoring grape ripening.
- Electrochemical signals on grapes at different ripening stages have been collected.
- Calibration models have been built for estimation of physicochemical parameters.
- Good predictive models have been obtained for pH, acidity, sugars and anthocyanins.

*Graphical Abstract (for review)

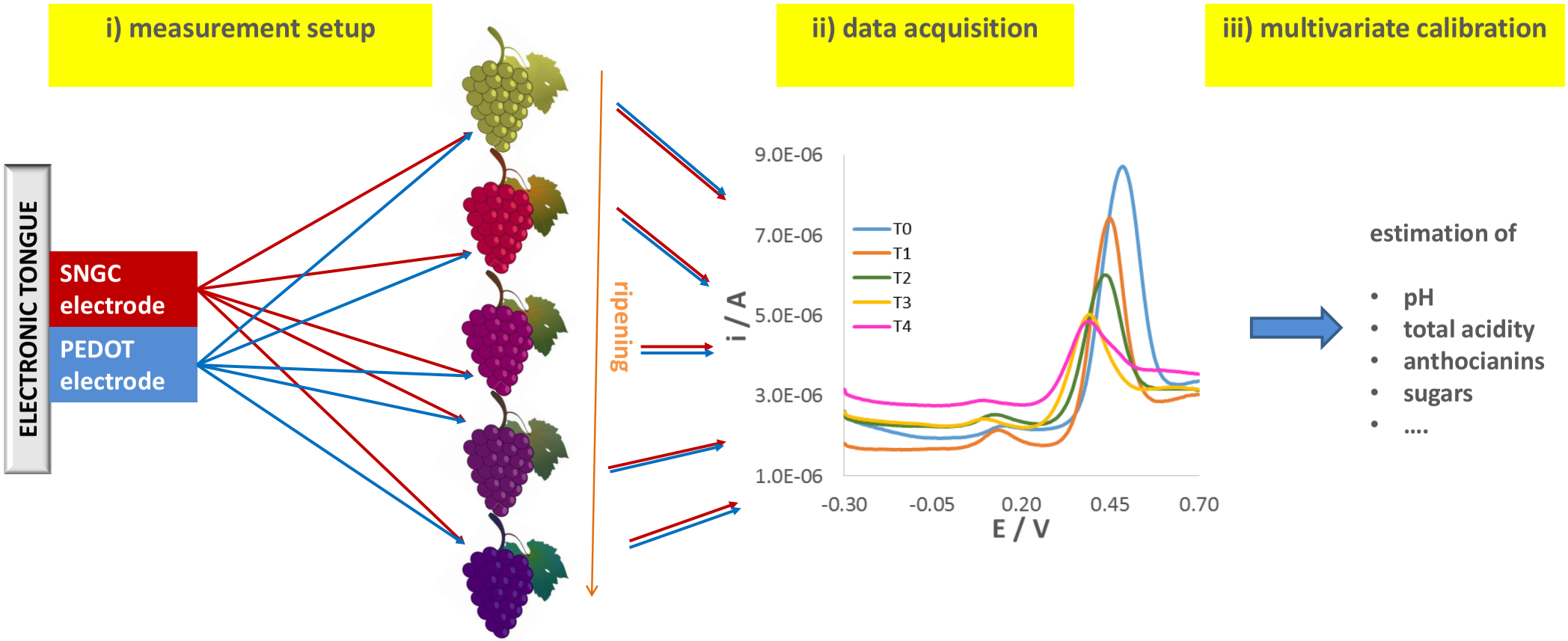

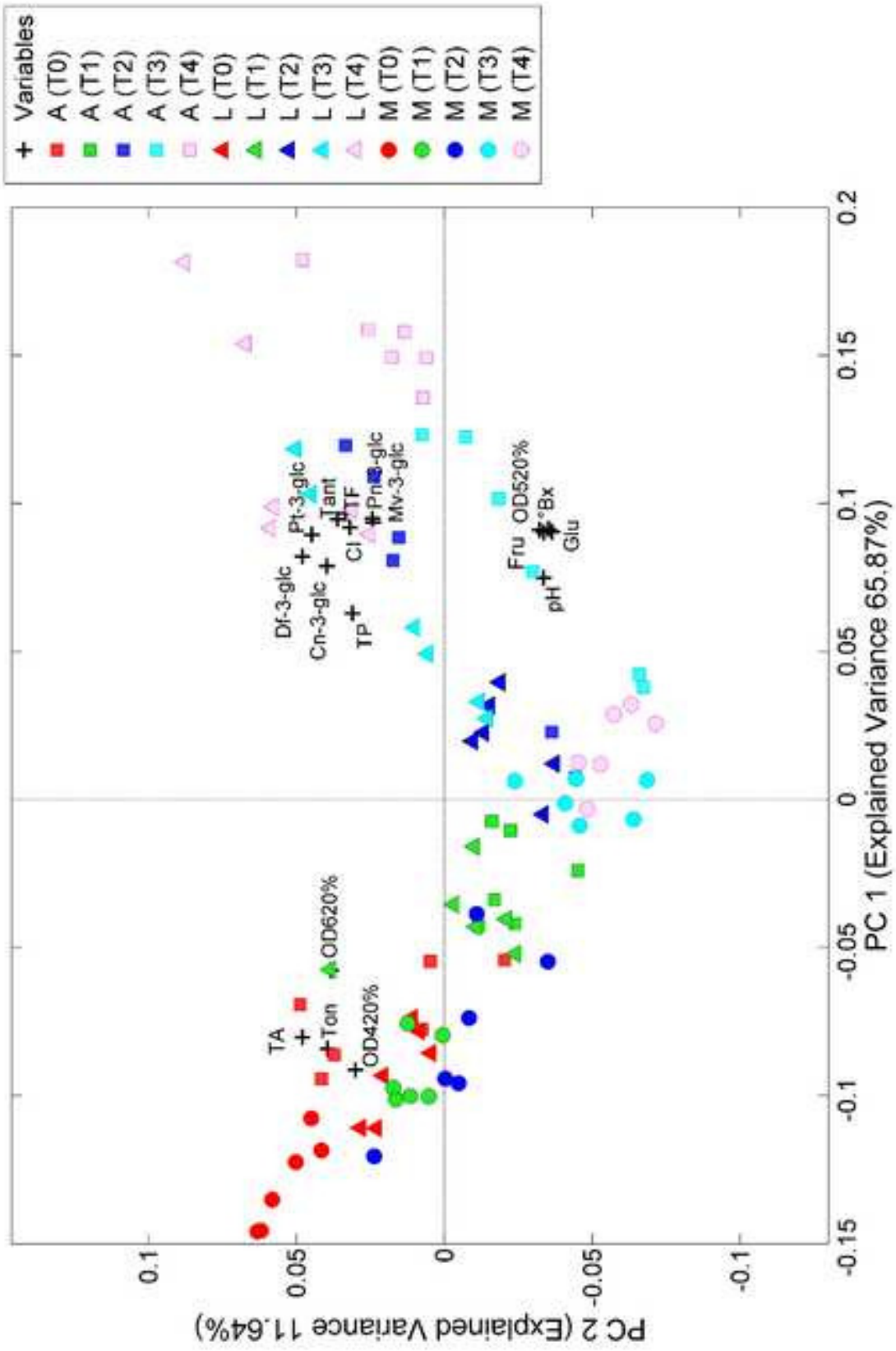


Figure 1

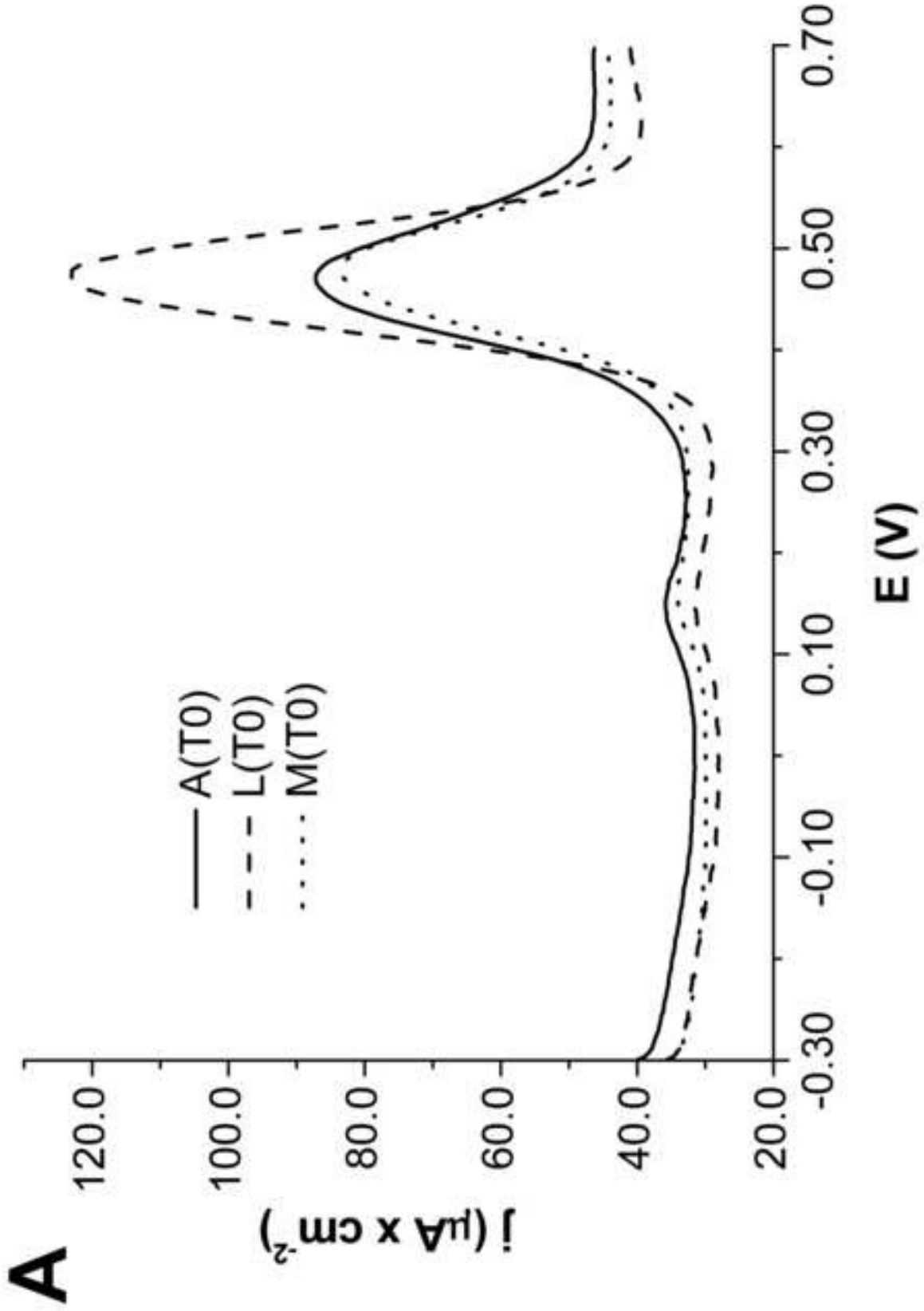
A
j (μA x cm⁻²)
120.0
100.0
80.0
60.0
40.0
20.0
-0.30
-0.10
0.10
0.30
0.50
0.70
E (V)
A(T0)
L(T0)
M(T0)

Figure 2 A

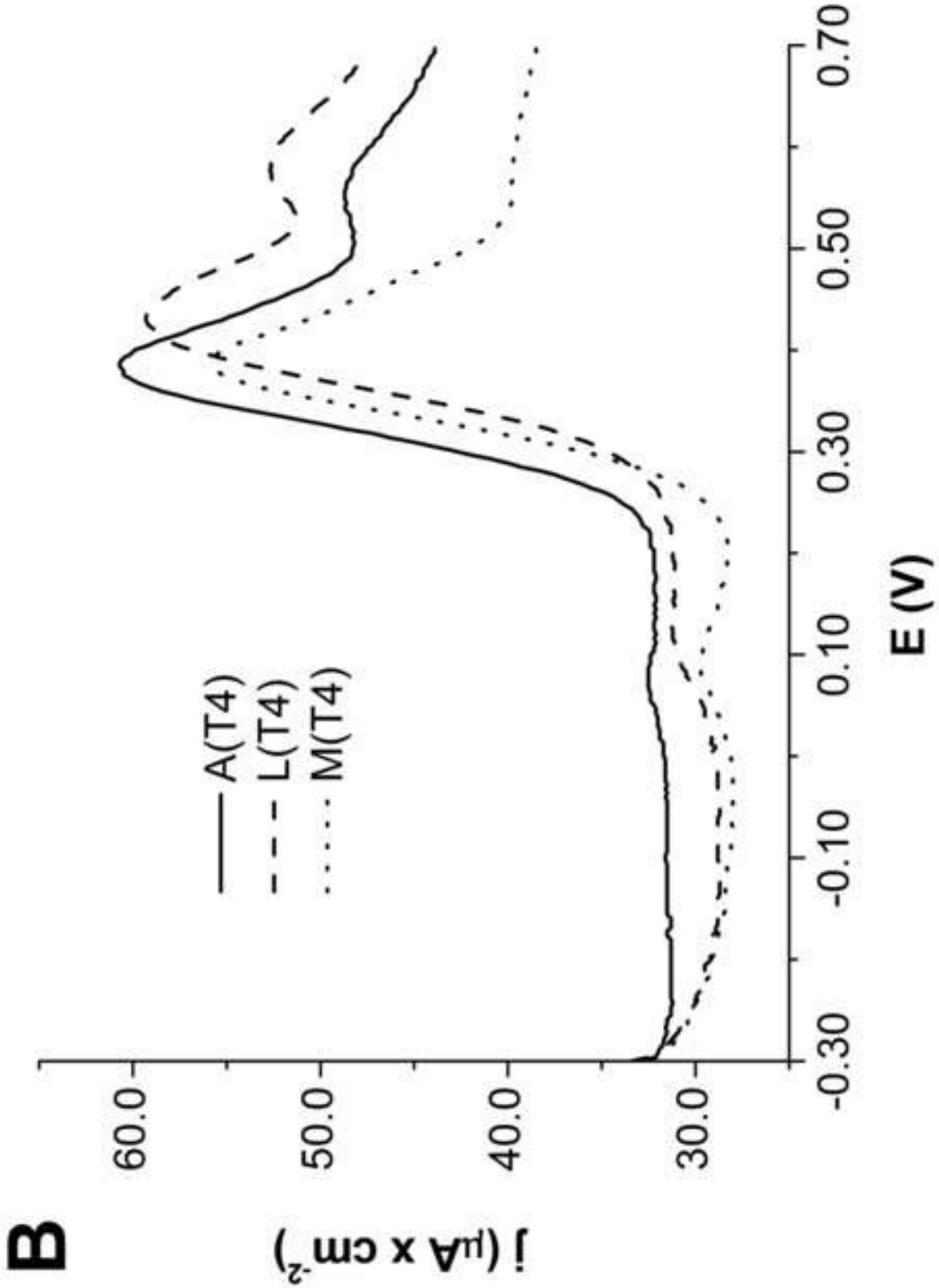


Figure 2 B

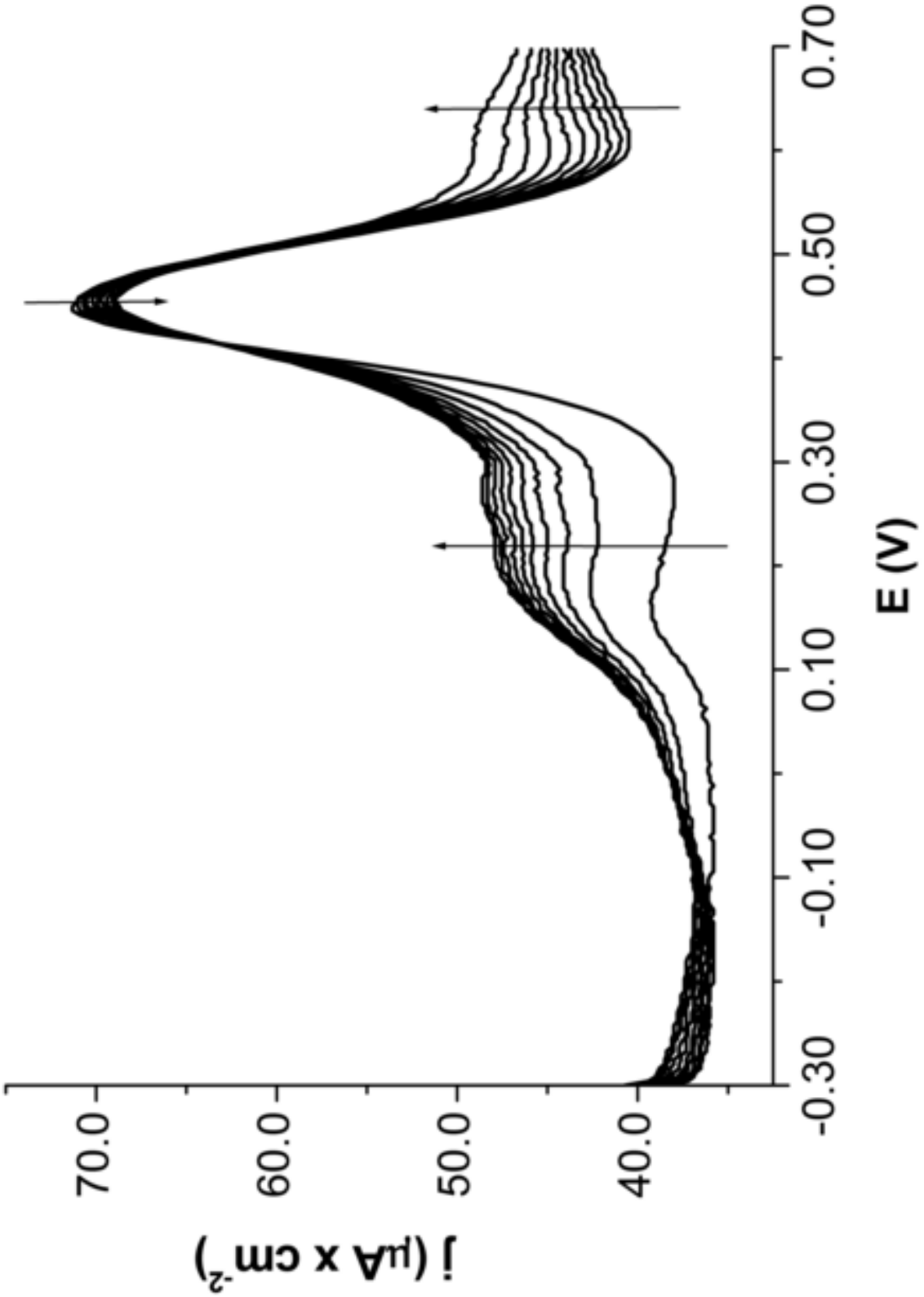


Figure 3

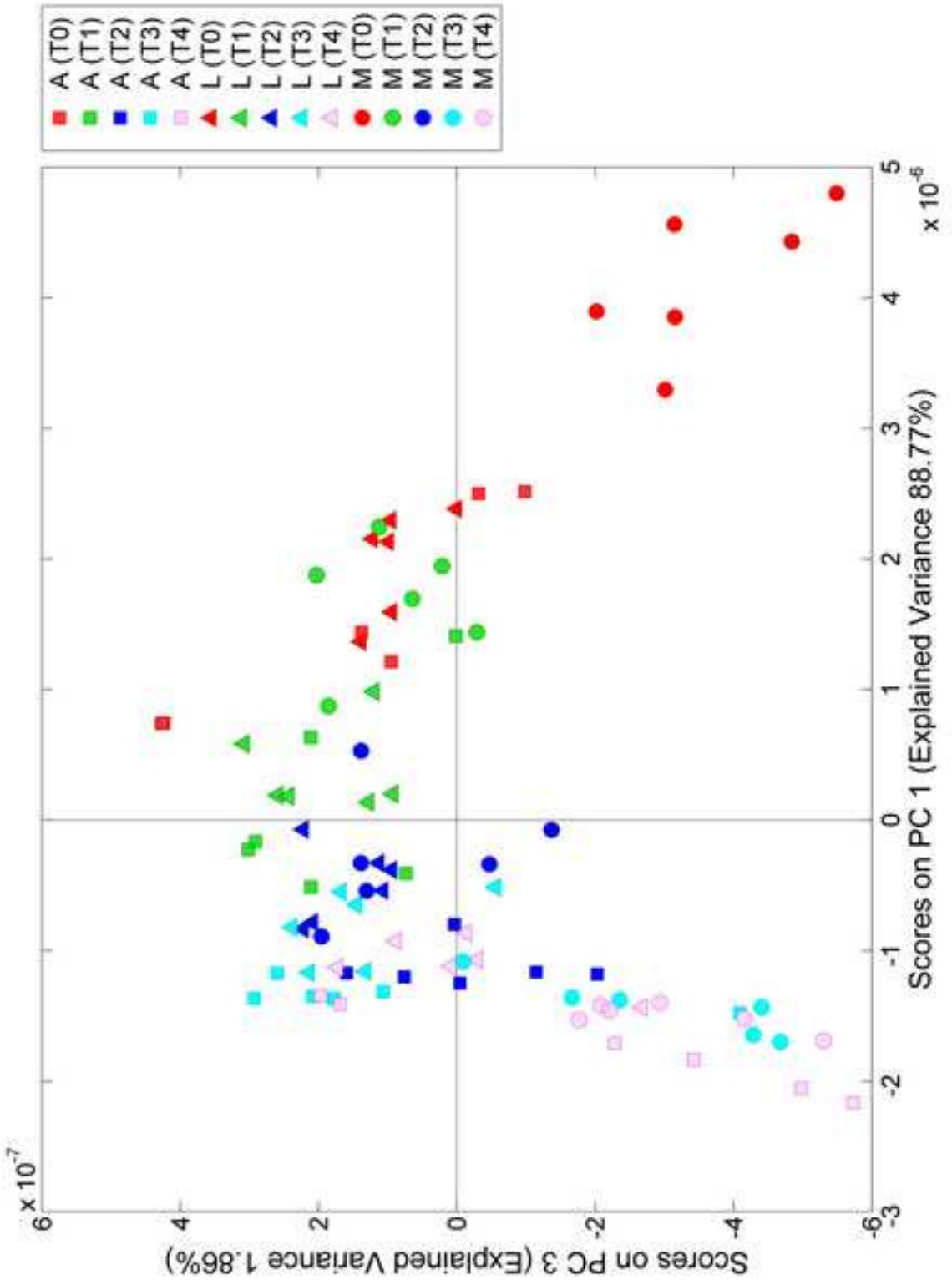
A (T0)
A (T1)
A (T2)
A (T3)
A (T4)
L (T0)
L (T1)
L (T2)
L (T3)
L (T4)
M (T0)
M (T1)
M (T2)
M (T3)
M (T4)
Scores on PC 1 (Explained Variance 88.77%)
x 10^-6
Scores on PC 3 (Explained Variance 1.86%)
x 10^-7

Figure 4

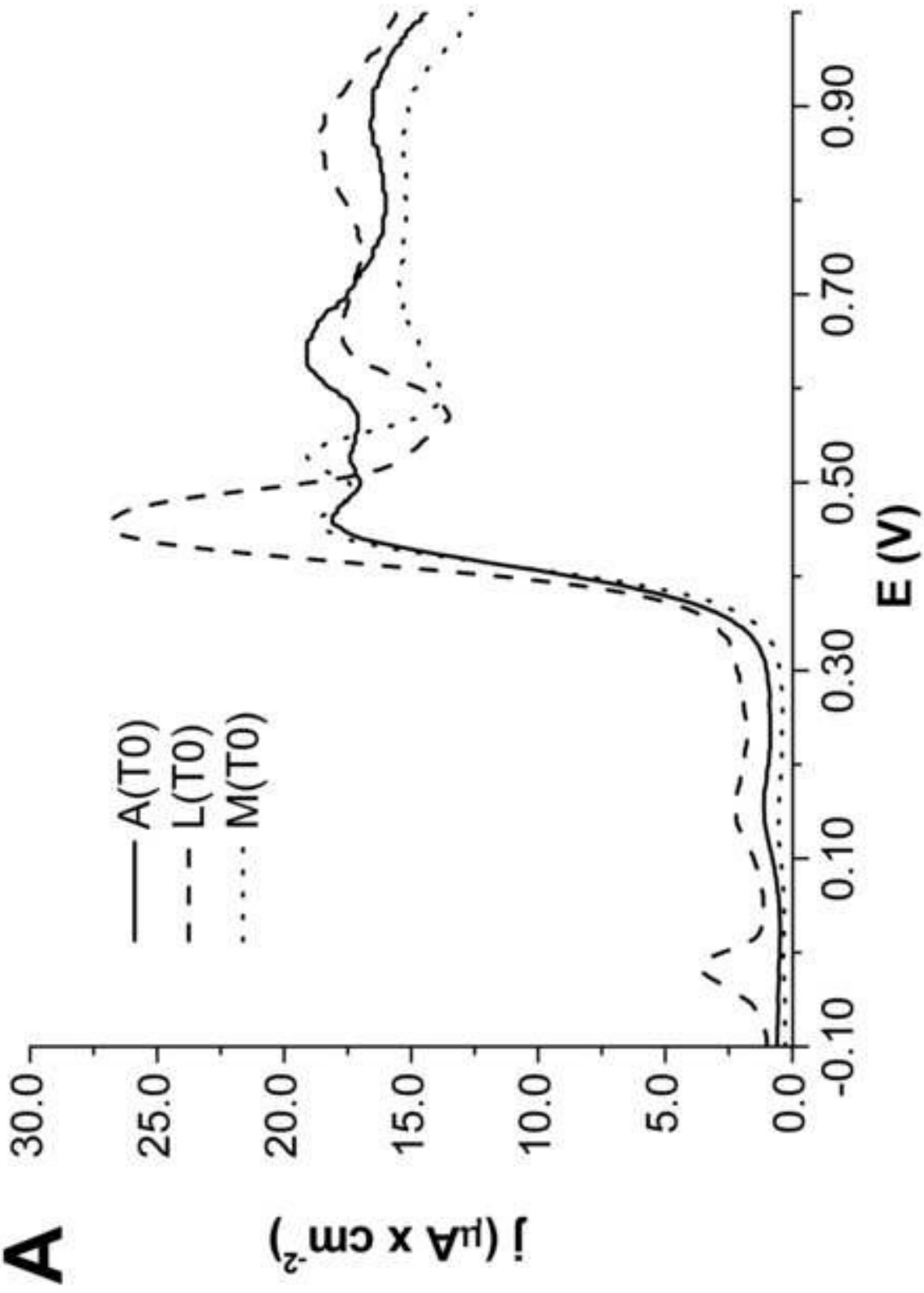
A
j (μA x cm⁻²)
30.0
25.0
20.0
15.0
10.0
5.0
0.0
-0.10
0.10
0.30
0.50
0.70
0.90
E (V)
A(T0)
L(T0)
M(T0)

Figure 5 A

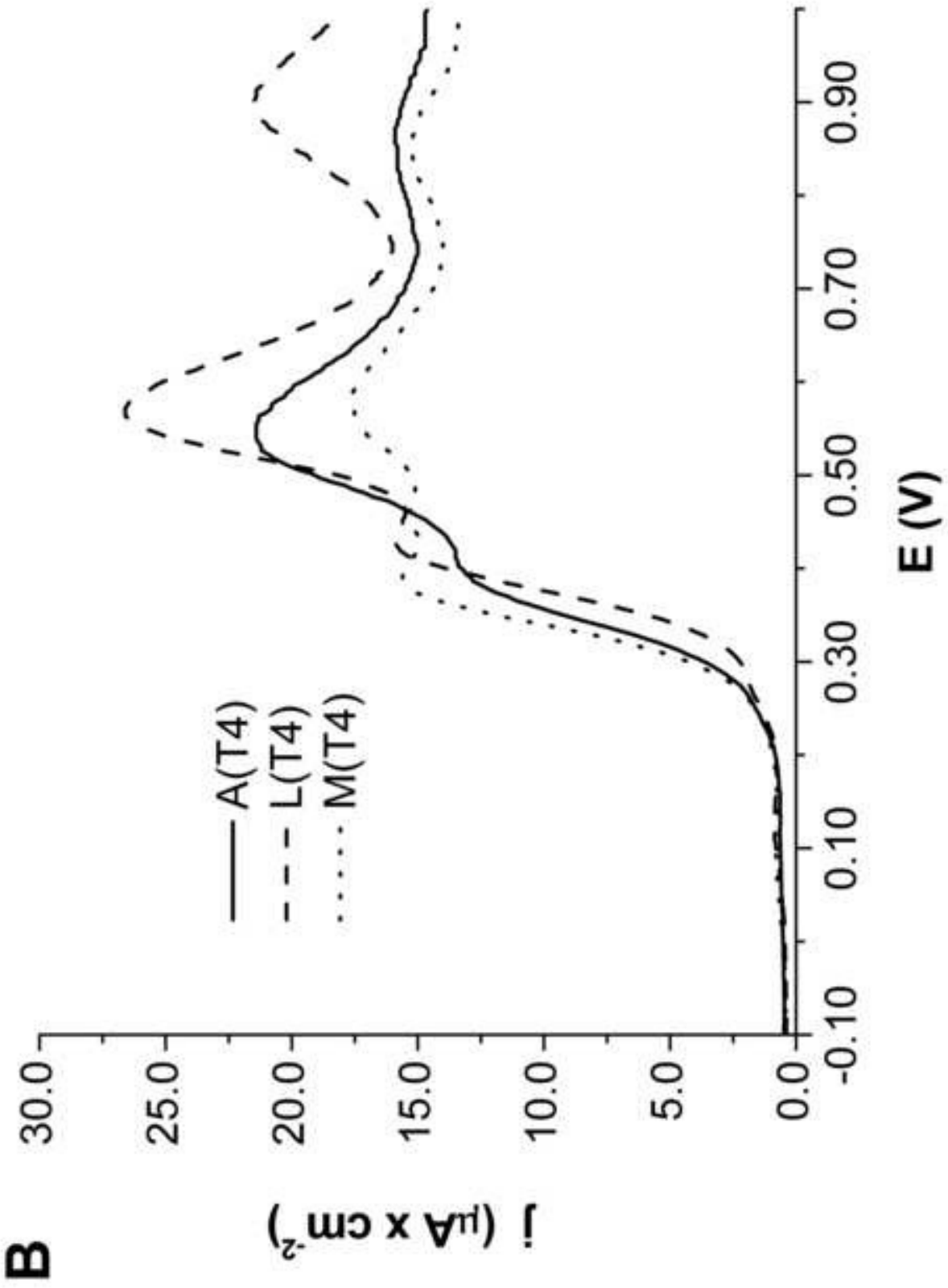


Figure 5 B

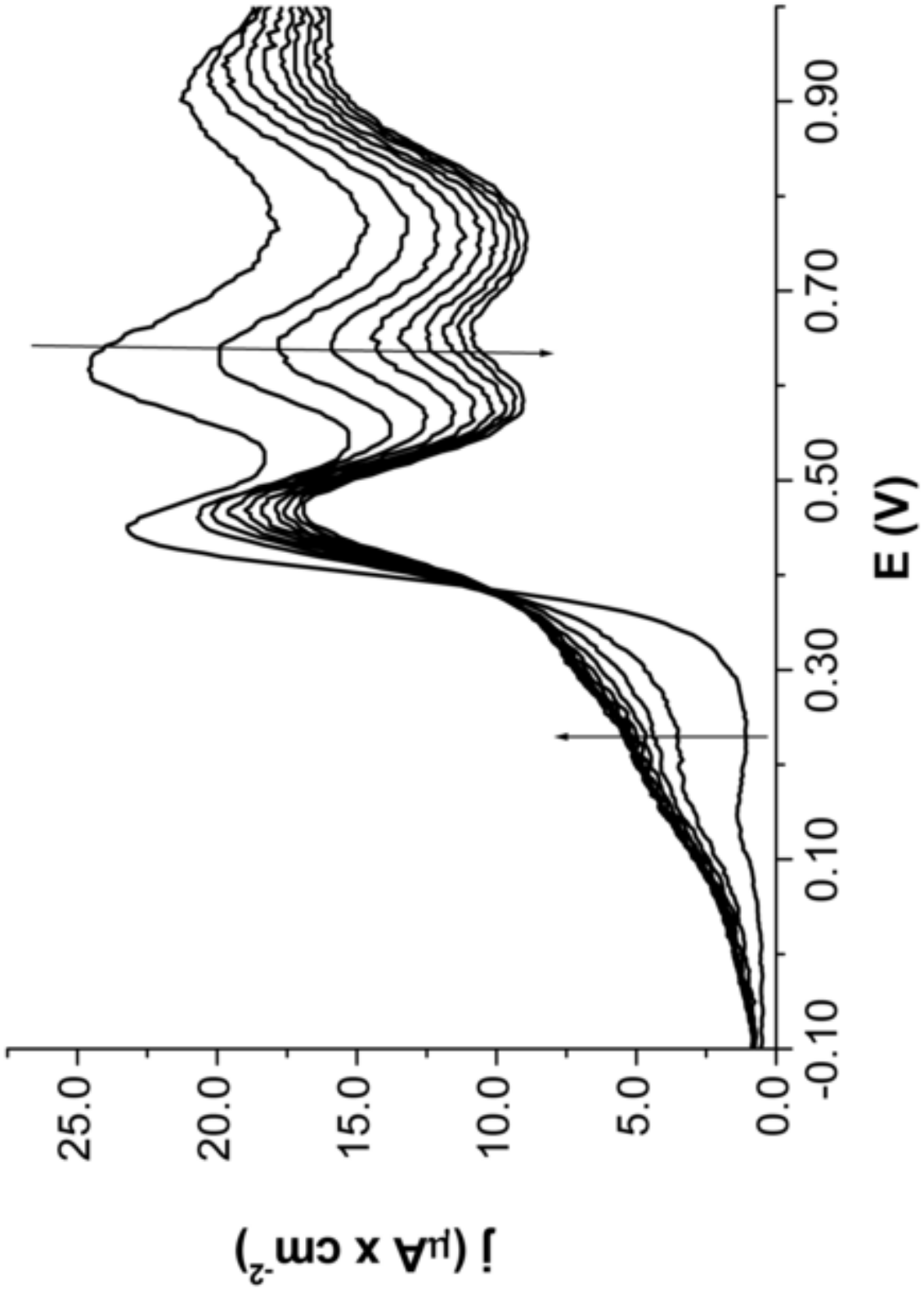


Figure 6

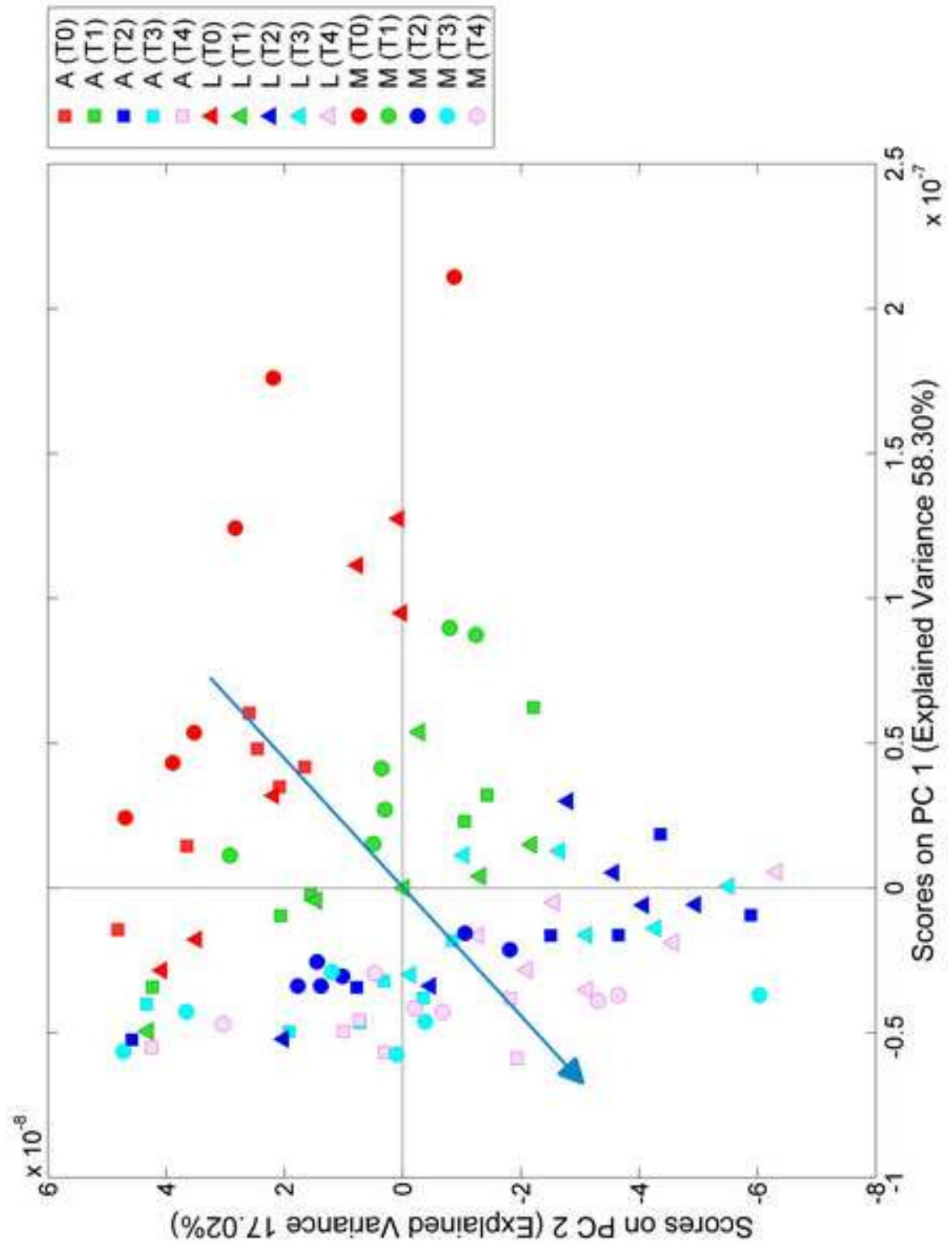
A (T0)
A (T1)
A (T2)
A (T3)
A (T4)
L (T0)
L (T1)
L (T2)
L (T3)
L (T4)
M (T0)
M (T1)
M (T2)
M (T3)
M (T4)
Scores on PC 1 (Explained Variance 58.30%)
x 10^-7
Scores on PC 2 (Explained Variance 17.02%)
x 10^-8

Figure 7